V. COMPOSITENESS

Contributors: E.N. Argyres, U. Baur, P. Chiappetta, C.G. Papadopoulos, M. Perrottet
M. Spira, S.D.P. Vlassopulos, P. Zerwas

V.1. Introduction

The proliferation of quarks and leptons and their mysterious deep relations among each other are suggestive indications for substructures of these particles [1]. No satisfactory theoretical model has been developed so far, in which the light masses of quarks and leptons could be reconciled with their small radii $< \mathcal{O}(10^{-16}$ cm) corresponding to a compositeness scale of 1 TeV and beyond. However, the quark model of hadrons has taught us very clearly in the past that theorists' puzzles cannot force Nature not to realize physically novel concepts. The compositeness scale may be anywhere between the $\mathcal{O}(1$ TeV) range and the Planck scale. A high–energy collider like the LHC will be able to either discover preonic substructures or to improve the limits on quark radii down to $\mathcal{O}(10^{-17}$ cm) in a model independent way, an order of magnitude more than accessible now.

(i) Quark radii can be measured or bounded by studying jet production at large transverse momenta [2]. A surplus of scattering events over the predictions from standard QCD would be observed at transverse momenta $p_\perp \sim \mathcal{O}(R^{-1})$ where the cross section would begin to be dominated by the non–pointlike quark radius R.

(ii) A unique signal for the substructure of quarks and leptons would be the discovery of excited states [3] towering over the lepton and quark ground states: $\ell, \ell^*, \ell^{**}, \ldots$ and $q, q^*, q^{**}, \ldots$ The masses m^* of excited fermions are generally expected to be of the order of the compositeness scale Λ.

We will not discuss a specific model in the following, but we will elaborate the experimental consequences of these two rather general physical points for the LHC. The main results of this study may be summarized in limits of $\sim$ 20 TeV for the compositeness scale probed in quark–quark scattering, and mass limits of 5 to 10 TeV for the production of excited leptons and quarks.

Other signatures of compositeness — strongly produced multi–lepton final states, lepto-quarks, colored leptons and other novel particle types — have been discussed frequently in the literature, see e.g. [1].

Compositeness of gauge bosons and Higgs particles can stabilize the Higgs mass. The natural scale of this sector is the Fermi scale $\sim$ 250 GeV. Substructures of these particles would manifest themselves through excited W^* and Z^* bosons and isoscalar partners which have been described elsewhere in this report. Anomalous production of gauge boson pairs due to non–standard trilinear self–couplings is another signal of substructures at distances of $\mathcal{O}(10^{-16}$ cm).

V.2. Bounds on Quark and Lepton Radii

Contributors: P. Chiappetta and M. Perrottet

The aim of this report is to study some effects of contact terms due to composite quarks and leptons on inclusive jet production and on massive dilepton production [4].

V.2.1. Inclusive jet production.

We first compute the effect of the 4 quark contact term of dimension 6 [5]

$$\mathcal{L}_{qqqq} = \frac{\eta g^2}{2\Lambda_q^2} \bar{\psi}_q^L \gamma^\mu \psi_q^L \bar{\psi}_q^L \gamma_\mu \psi_q^L \tag{1}$$

on the inclusive one jet production at $\sqrt{s} = 16$ TeV (LHC) and $\sqrt{s} = 40$ TeV (SSC). Here η is a sign $(\pm 1), g$ a strong interaction coupling constant such that $g^2 = 4\pi$ and Λ_q is the compositeness scale associated with the effective 4 quark operator of eq. (1). ψ_q^L is the usual $SU(2)_L$ doublet made out of up- and down-type quarks. Note that the current in the current-current interaction (1) is a color- and isospin-singlet. More precisely, we study the deviations due to (1), with respect to the lowest order QCD predictions, on the differential cross section

$$\frac{d^2\sigma}{dp_T dy}\Big|_{y=0} \tag{2}$$

where p_T is the jet transverse momentum and y is rapidity. The contact term (1) modifies the various elementary two-body quark cross sections. Because we disagree with some of the results published by other authors [5,7], we give below a list of our own formulas

$$q_i\bar{q}_j \to q_i\bar{q}_j : |\mathcal{M}|^2 = \frac{4}{9}\frac{\hat{u}^2 + \hat{s}^2}{\hat{t}^2} + \hat{u}^2 C^2 \tag{3}$$

$$q_i q_j \to q_i q_j : |\mathcal{M}|^2 = \frac{4}{9}\frac{\hat{u}^2 + \hat{s}^2}{\hat{t}^2} + \hat{s}^2 C^2 \tag{4}$$

$$q_i\bar{q}_i \to q_j\bar{q}_j : |\mathcal{M}|^2 = \frac{4}{9}\frac{\hat{u}^2 + \hat{t}^2}{\hat{s}^2} + \hat{u}^2 C^2 \tag{5}$$

$$\bar{q}_i\bar{q}_j \to \bar{q}_i\bar{q}_j : |\mathcal{M}|^2 = \frac{4}{9}\frac{\hat{u}^2 + \hat{s}^2}{\hat{t}^2} + \hat{s}^2 C^2 \tag{6}$$

$$q_i q_i \to q_i q_i : |\mathcal{M}|^2 = \frac{4}{9}\left\{\frac{\hat{s}^2 + \hat{u}^2}{\hat{t}^2} + \frac{\hat{s}^2 + \hat{t}^2}{\hat{u}^2} - \frac{2}{3}\frac{\hat{s}^2}{\hat{u}\hat{t}}\right\} + \frac{8}{9}\hat{s}^2\left(\frac{1}{\hat{t}} + \frac{1}{\hat{u}}\right)C + \frac{8}{3}\hat{s}^2 C^2 \tag{7}$$

$$q_i\bar{q}_i \to q_i\bar{q}_i : |\mathcal{M}|^2 = \frac{4}{9}\left\{\frac{\hat{u}^2 + \hat{s}^2}{\hat{t}^2} + \frac{\hat{u}^2 + \hat{t}^2}{\hat{s}^2} - \frac{2}{3}\frac{\hat{u}^2}{\hat{s}\hat{t}}\right\} + \frac{8}{9}\hat{u}^2\left(\frac{1}{\hat{t}} + \frac{1}{\hat{s}}\right)C + \frac{8}{3}\hat{u}^2 C^2 \tag{8}$$

$$\bar{q}_i\bar{q}_i \to \bar{q}_i\bar{q}_i : |\mathcal{M}|^2 = \frac{4}{9}\left\{\frac{\hat{s}^2+\hat{u}^2}{\hat{t}^2} + \frac{\hat{s}^2+\hat{t}^2}{\hat{u}^2} - \frac{2}{3}\frac{\hat{s}^2}{\hat{u}\hat{t}}\right\} + \frac{8}{9}\hat{s}^2\left(\frac{1}{\hat{t}}+\frac{1}{\hat{u}}\right)C + \frac{8}{3}\hat{s}^2C^2 \qquad (9)$$

The indices i and j refer to quark flavors. $\hat{s}, \hat{t}$ and $\hat{u}$ are the usual Mandelstam variables. C is directly related to the compositeness scale Λ_q through

$$C = \frac{\eta}{\alpha_s(Q^2)\Lambda_q^2} \quad . \qquad (10)$$

Finally, the differential cross sections $d\sigma/d\hat{t}$ which enter into the computation of eq. (2) are given by

$$\frac{d\sigma}{d\hat{t}} = \frac{\pi}{\hat{s}^2}\alpha_s^2(Q^2)|\mathcal{M}|^2 \qquad (11)$$

where the argument Q^2 of the effective QCD coupling constant is p_T^2. In order to obtain results which are little sensitive to the choice of structure functions and mass scales, we have studied the ratio

$$D = \frac{\frac{d^2\sigma}{dp_Tdy}\Big|_{y=0}(\text{QCD + CT}) - \frac{d^2\sigma}{dp_Tdy}\Big|_{y=0}(\text{QCD})}{\frac{d^2\sigma}{dp_Tdy}\Big|_{y=0}(\text{QCD})} \qquad (12)$$

where CT means contact term. The discovery limits for the compositeness scale Λ_q that we will give below correspond to a deviation from the QCD prediction larger than 100%, namely $D \geq 1$ (theoretical uncertainties including higher order corrections are of the order of 40% [8]). With $\Delta p_T = 100\text{GeV/c}$, we would like to have at least ten events per year in the standard model. Considering the expected luminosities $\mathcal{L}_{\text{LHC}} = 10^{34}cm^{-2}s^{-1}$ and $\mathcal{L}_{\text{SSC}} = 10^{33}cm^{-2}s^{-1}$, one can reach for the cross section (2) $x_T \equiv \frac{2p_T}{\sqrt{s}} \cong 0.5$ for LHC, and $x_T \cong 0.3$ for SSC.These discovery limits are displayed in table 1 for LHC and SSC, using two sets of distribution functions, DFLM set of ref. [9] with $\Lambda_{QCD} = 160$ MeV, and set 1 of Duke-Owens [10]. As expected, there is little sensitivity to the choice of structure functions, typically a few percent. It should be noted that the difference in luminosities compensates to a large extent the gap in energy between LHC and SSC. We have checked that another choice of the mass scale ($Q^2 = p_T^2/4$) changes the discovery limits by a few percent only.

Table 1

	qqqq CT		qqgg CT	
	$\eta = +1$	$\eta = -1$	Vector	Axial
LHC Duke–Owens	20 TeV	28 TeV	4.6 TeV	4.6 TeV
LHC Diemoz et al.	20 TeV	27 TeV	4.3 TeV	4.4 TeV
SSC Duke–Owens	27 TeV	33 TeV	7.6 TeV	7.7 TeV
SSC Diemoz et al.	27 TeV	32 TeV	7.4 TeV	7.5 TeV

Obviously discovery limits depend on luminosity and the value of required deviation from QCD prediction. As an example if we assume $\mathcal{L}_{LHC} = 10^{33}cm^{-2}sec^{-1}$ and a deviation larger than 200 % we get a discovery limit of 13 TeV for $\eta = +1$. We have also computed the effect

of a contact term between transverse gluons considered as true gauge particles and composite quarks. Several CP- and chirality-conserving operators can be written [11] but for the present study we have selected the one of the lowest dimension. It is called N_{TT}^2 in ref. [11] and can be written as [12]

$$\mathcal{L}_{qqgg} = i\frac{\alpha_s}{\Lambda_g^4}\bar{\psi}_q\left\{(\gamma^\mu\partial_\rho + \gamma_\rho\partial^\mu)(C_V - C_A\gamma_5)\psi_q\right\}G_{\mu\nu}G^{\nu\rho} \tag{13}$$

where Λ_g is the compositeness scale associated with the dimension 8 operator, $C_V(C_A)$ the vector (axial) part of the lagrangian. For completeness, we give below the contribution of (13) to the relevant processes [6]

$$q_i\bar{q}_i \to gg : |\mathcal{M}|^2 = \frac{8}{3}\left(\hat{u}^2+\hat{t}^2\right)\left\{\frac{4}{9\hat{u}\hat{t}} - \frac{1}{\hat{s}^2}\right\} + \frac{4}{3}\frac{\hat{u}^2+\hat{t}^2}{\Lambda_g^4}\left\{\frac{2}{3}C_V + \frac{\hat{u}\hat{t}}{\Lambda_g^4}\left(C_V^2+C_A^2\right)\right\} \tag{14}$$

$$q_ig \to q_ig : |\mathcal{M}|^2 = -\left(\hat{u}^2+\hat{s}^2\right)\left\{\frac{4}{9\hat{u}\hat{s}} - \frac{1}{\hat{t}^2}\right\} - \frac{1}{2}\frac{\hat{u}^2+\hat{s}^2}{\Lambda_g^4}\left\{\frac{2}{3}C_V + \frac{\hat{u}\hat{s}}{\Lambda_g^4}\left(C_V^2+C_A^2\right)\right\} \tag{15}$$

$$gg \to q_i\bar{q}_i : |\mathcal{M}|^2 = \frac{3}{8}\left(\hat{u}^2+\hat{t}^2\right)\left\{\frac{4}{9\hat{u}\hat{t}} - \frac{1}{\hat{s}^2}\right\} + \frac{3}{16}\frac{\hat{u}^2+\hat{t}^2}{\Lambda_g^4}\left\{\frac{2}{3}C_V + \frac{\hat{u}\hat{t}}{\Lambda_g^4}\left(C_V^2+C_A^2\right)\right\} \quad . \tag{16}$$

We have assumed that the color structure in the contact term is the same as that of the QCD amplitude. The differential cross section $d\sigma/d\hat{t}$ is still given by eq. (11). Since QCD is a vector theory, the interference term between QCD and the contact interaction (13) is simply proportional to the vector coupling C_V. To set discovery limits for the compositeness scale Λ_g, we used the same approach as for interaction (1). These limits are given in Table 1. There is little difference between the vector case ($C_V = 1, C_A = 0$) and the axial one ($C_V = 0, C_A = 1$). Of course, the operator (13) being of higher dimension than (1), the discovery limits are much lower and will be completely hidden by the presence of the contact term (1) if one assumes that Λ_q is of the order of Λ_g.

V.2.2. Massive lepton pair production

Finally, we have similarly analyzed the influence of a contact term between quarks and leptons on massive dilepton production through the Drell-Yan mechanism. The effective contact interaction is similar to (1)

$$\mathcal{L}_{qqll} = \frac{\eta g^2}{4\Lambda_{lq}^2}\bar{\psi}_l\gamma^\mu(1-\eta_l\gamma_5)\psi_l\bar{\psi}_q\gamma_\mu(1-\eta_q\gamma_5)\psi_q \tag{17}$$

with $\eta = \pm 1, \eta_l = \pm 1, \eta_q = \pm 1, g^2 = 4\pi$ and Λ_{lq} is the compositeness scale associated to the dimension 6 operator of eq. (17). We will use the same criteria as described previously to define the discovery limits, namely deviations with respect to the QCD predictions larger than 100%.

We will concentrate on the differential cross section $\frac{d\sigma}{dM_{l^+l^-}}$ where $M_{l^+l^-}$ is the invariant mass of the lepton pair. Then the deviation to study is

$$\tilde{D} = \frac{\frac{d\sigma}{dM_{l^+l}}(\text{QCD} + \text{CT}) - \frac{d\sigma}{dM_{l^+l^-}}(\text{QCD})}{\frac{d\sigma}{dM_{l^+l^-}}(\text{QCD})} \tag{18}$$

where CT is now the contribution from the interaction (17). Keeping in mind a rate of at least 10 events per year from the standard model with $\Delta M = 100\text{GeV}$, a direct computation shows that one can reach $M_{l^+l^-} \cong 2.05\text{TeV}$ at LHC and $M_{l^+l^-} \cong 2.15\text{TeV}$ at SSC. For illustration, we have considered the two extreme chirality cases $\eta_l = \eta_q = 1$ (left-left, or LL) and $\eta_l = \eta_q = -1$ (right-right or RR). The corresponding discovery limits are displayed in Table 2 for LHC and SSC with the structure functions of ref. [9]. One can see that the difference in luminosity between LHC and SSC compensates exactly the difference in energy. We can also notice that for a given overall sign of the contact interaction (17), the discovery limits depend very little on the choice of chirality (LL or RR).

Table 2

	$\eta = +1$		$\eta = -1$	
	LL	RR	LL	RR
LHC	15 TeV	16 TeV	25 TeV	25 TeV
SSC	15 TeV	16 TeV	24 TeV	24 TeV

V.2.3. Conclusion

To conclude, it is interesting to make a comparison between our results and the corresponding limits at Hera and at the Tevatron. For Hera, the LL 2quark- 2lepton contact term (17) leads to a discovery limit of about 5 TeV [13], to be compared with the 15 TeV limit of Table 2. Concerning the 4 quark contact term (1), LHC and SSC will improve the expected Tevatron limit (2 to 3 TeV) [14] by roughly one order of magnitude.

V.3. Testing Contact Interactions of Quarks and Gluons at Future pp Colliders

Contributors: E.N.Argyres, C.G.Papadopoulos and S.D.P.Vlassopulos

New interactions at an energy scale Λ of the order of a few TeV will manifest themselves at energies below this scale, through deviations from the Standard Model (SM), described by an effective non-renormalizable $SU(3) \otimes SU(2) \otimes U(1)$ invariant lagrangian. Such interactions may arise either as low-energy tails of heavy exotic particle exchange (e.g. non-minimal Higgses, E_6-diquarks, extra neutral currents, etc) or as a manifestation of quark and gluon substructure. It is therefore, interesting to search for deviations from the SM predictions at future accelerators, like LHC and SSC, which will provide us with the highest available center of mass energies, $\sqrt{s}$ =16TeV and 40TeV, respectively.

In this work we calculate the effect of qq,qg,gg contact interactions, described by [15]

$$\mathcal{L}_{eff} = g_1 f_{ABC} G_\mu^{A\nu} G_\nu^{B\lambda} G_\lambda^{C\mu} \tag{19a}$$

$$+ i g_2 \bar{q} \lambda^A \gamma_\mu D_\nu q G^{A\mu\nu} \tag{19b}$$

$$+ i g_3 \bar{q} \gamma_\mu q \bar{q} \gamma^\mu q \tag{19c}$$

$$+ i g_4 \bar{q} \lambda^A \gamma_\mu q \bar{q} \lambda^A \gamma^\mu q \tag{19d}$$

in the 2- and 3-jet cross sections. The dimensionful coupling constants, g_i, are given by $g_i = \eta_i \frac{4\pi}{\Lambda^2}$, where $\eta_i = \pm 1$ and we have assumed a common scale Λ. More explicitly we calculate

$$\sigma(pp \to \text{n jets} + \text{X}) = \int \sum_{a,b} dx_a dx_b \mathcal{F}_a(x_a, Q) \mathcal{F}_b(x_b, Q) \mid \mathcal{M}_{ab} \mid^2 d\mathcal{L}ips^{(n)} \tag{20}$$

where $\mathcal{F}_a$ are the quark and gluon distributions and $\mathcal{M}_{ab}$ the helicity amplitudes, calculated using the "E-product" [16] formulation of the well known spinor-product technique [17]. Notice that in the case $n = 2$ the full lagrangian (19) has been used, whereas in the case $n = 3$ only the operator (19c) has been employed[4]. In both cases we use $\eta_i = +1$.

In order to compare the theoretical predictions with experimental data we have to impose appropriate cuts on the momenta of the produced jets, quarks and gluons, which, neglecting all hadronization effects, are simply

$$\mid \eta_{\text{jet}} \mid \leq 2.5 \tag{21a}$$

$$\cos(\theta_{ij}) \leq 0.766 \ (\theta_{min} = 40^0) \tag{21b}$$

where η_{jet} is the pseudorapidity and θ_{ij} the angle between the 3-momenta of the jets i and j. We use $Q = \sqrt{\hat{s}}$, $\hat{s} = x_a x_b s$ and the structure-function parametrization EHLQ II [18] with $\Lambda_{\text{QCD}} = 0.29\text{GeV}$.

Since we are interested in enhancing the signal of the new interactions, we impose the supplementary cuts

$$M_{\text{njets}} \geq 6.4(12)\text{TeV} \tag{22a}$$

$$p_T \geq 0.4(1)\text{TeV} \tag{22b}$$

for $\sqrt{s} = 16(40)\text{TeV}$, where M_{njets} is the invariant mass of the produced jets [19] and p_T the transverse momentum. These cuts have the effect to suppress the QCD background, whereas the contact interaction contribution remains almost unaffected. Notice that the cuts (22a) and (22b) are necessary in the case $n = 3$, since a quark-quark contact interaction signal can be detectable only if we suppress the gg initial state contribution [19]. We focus our attention to the normalized χ distribution,

$$\frac{1}{\sigma} \frac{d\sigma}{d\chi}$$

where

$$\chi = \frac{1 + \cos\theta^*}{1 - \cos\theta^*} \tag{23}$$

[4]The details of the calculation will be given elsewhere

and θ^* is the c.m. angle of the beam and the produced jet momentum, in the 2-jet case, and the angle of the beam with the fastest jet, in the 3-jet case.

Figs.(1a) and (1b) show the 2-jet cross section for $\sqrt{s} = 16$ and 40 TeV respectively. As we can see, the contact interaction prefers to accumulate events at smaller values of χ (spherical events), whereas the QCD background is almost flat. If one assumes a statistical error

$$\frac{\delta\sigma}{\sigma} = \sqrt{\frac{1}{\sigma\mathcal{L}}} \tag{24}$$

where $\mathcal{L}$ is the luminosity , a χ^2 analysis gives that (at 95% C.L.):

$$\Lambda \geq 40\text{TeV}(\sqrt{s} = 16\text{TeV}) \tag{25a}$$

$$\Lambda \geq 50\text{TeV}(\sqrt{s} = 40\text{TeV}) \tag{25b}$$

where we have used $\mathcal{L} = 400\text{fb}^{-1}$ at LHC and $\mathcal{L} = 10\text{fb}^{-1}$ at SSC [20].

In figs.(2a) and (2b) we show the results for the three-jet cross section. The corresponding bounds are:

$$\Lambda \geq 15\text{TeV}(\sqrt{s} = 16\text{TeV}) \tag{26a}$$

$$\Lambda \geq 10\text{TeV}(\sqrt{s} = 40\text{TeV}) \tag{26b}$$

The bound for the SSC is smaller than for the LHC, due to the smaller luminosity of the SSC and to the fact that the 3-jet χ-distribution of QCD is not flat.

Although there are other quantities which are sensitive to contact interactions, like the p_T spectrum, the normalized χ distribution offers the very advantage of being relatively free of the uncertainties due to the small-x behaviour of the gluon distribution and the higher order QCD corrections (in particular, choice of the scale Q^2 and the jet-cone size) [8], which are expected not to be strongly dependent on χ.

Comparing the bounds in all cases, one can state, that the luminosity $\mathcal{L}$ is a crucial parameter in order to probe the contact interactions. Especially for the quark-quark contact interactions, LHC seems to be more sensitive than SSC.

V.4. Excited Quarks and Leptons

Contributors: U. Baur, M. Spira and P. Zerwas

Spin and isospin of the excited fermions will be set to 1/2 in order to restrict the number of parameters to be introduced in this study [3]. The assignment of left- and right-handed components to isodoublets, e.g. for the first generation

$$\begin{bmatrix} \nu_e \\ e^- \end{bmatrix}_L \quad \nu_{eR} \quad \begin{bmatrix} \nu_e^* \\ e^{*-} \end{bmatrix}_L \quad \begin{bmatrix} \nu_e^* \\ e^{*-} \end{bmatrix}_R \quad \text{and} \quad \begin{bmatrix} u \\ d \end{bmatrix}_L \quad u_R \quad \begin{bmatrix} u^* \\ d^* \end{bmatrix}_L \quad \begin{bmatrix} u^* \\ d^* \end{bmatrix}_R$$

allows for non-zero masses prior to $SU(2) \times U(1)$ symmetry breaking, and it protects $(g-2)_\ell$ quadratically in the mass ratio $(m_\ell/m^*)^2$. The coupling of excited fermion states to the chiral Standard Model particles consists of three interaction types:

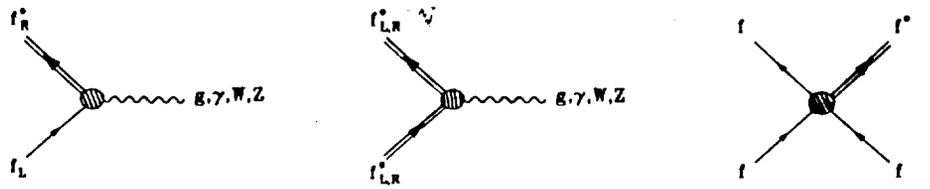

the first being the standard fermion–gauge boson interaction; the second being a gauge invariant magnetic type coupling between ground state and excited state; the third describing the strong excitation of fermions through contact interactions mediated, for instance, by preon interchange. Throughout this analysis we put $m^* = \Lambda$, for the sake of simplicity, and we neglect [minor] form factor effects.

Decay. Heavy excited fermions will decay into light fermions plus gauge bosons, but also, through preon–pair creation, into bunches of quarks and leptons

$$f^* \to f + V \qquad \text{and} \qquad f^* \to f + f'\bar{f}'$$

with $V = g,\ \gamma,\ Z,\ W$. Assuming $m^* \gg m_{W,Z}$ and neglecting light quark masses, the partial widths for the various gauge decay channels lead to the branching ratios listed in Table 3.

Table 3

	$\sum_V \Gamma(f^* \to fV)/m^*$ $[m^* = \Lambda]$
ν^*	$6.5 \cdot 10^{-3}$
e^*	$6.5 \cdot 10^{-3}$
u^*	$3.9 \cdot 10^{-2}$
d^*	$3.9 \cdot 10^{-2}$

e^*	B_G
$e\gamma$	0.28
eZ	0.11
νW	0.61

ν^*	B_G
νZ	0.39
eW	0.61

u^*	B_G
ug	0.85
$u\gamma$	0.02
uZ	0.03
dW	0.10

d^*	B_G
dg	0.85
$d\gamma$	0.005
dZ	0.05
uW	0.10

Contact interactions widen the excited states such that excited leptons and quarks would have comparable widths as expected from strong preon interactions. Results are shown in Table 4.

Table 4

	Γ_{tot}/m^*	Γ_G/Γ_{tot}	Γ_{CT}/Γ_{tot}	leptonic decays/all
ν^*	$8.9 \cdot 10^{-2}$	0.07	0.93	100%
e^*	$8.9 \cdot 10^{-2}$	0.07	0.93	100%
u^*	$1.2 \cdot 10^{-1}$	0.32	0.68	16.3%
d^*	$1.2 \cdot 10^{-1}$	0.32	0.68	16.3%

q^* production. Excited quarks can be produced in pp collisions through a variety of mechanisms. The dominant processes are the gluonic excitation of quarks $g + q \to q^*$ [3,21,22] and the excitation through contact interactions $qq \to qq^*$ [3,21].

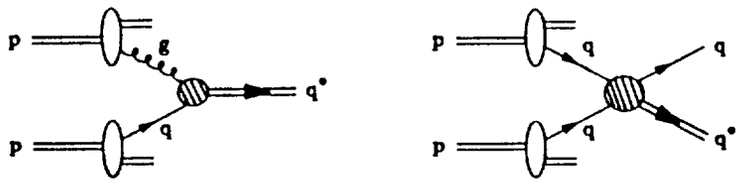

The cross section for the gluonic excitation of quarks, $qg \to q^*$, at pp colliders is shown in Fig. 3. Assuming gauge interactions to dominate over contact interactions, the signals for singly produced excited quarks are large transverse momentum jj, $j\gamma$, jZ or jW pairs with an invariant mass peaking at m^*. The jj mass distributions of the QCD background is integrated over twice the q^* width. The mass distributions for pp collisions at $\sqrt{s} = 16$ TeV are shown in Fig. 4 for various values of m^*. At LHC the q^* signal stands out clearly. Similar results are obtained for $j\gamma$, jW and jZ final states.

If contact interactions contribute significantly to the decay rate of excited quarks they may be a bubbling source for excited quarks q^* at hadron colliders. Excited quarks can be produced through contact interactions in qq collisions and $q\bar{q}$ annihilation together with an ordinary quark. Excited quark decays, mediated either by gauge or contact interactions lead to final states that consist of three or four jets, two jets and a photon, or two jets and a lepton pair. The qq^* production cross sections for LHC energies are shown in Fig. 5. The background to the qq^* signal, the q^* decaying into three jets via contact interactions, are four-jet final states. In addition to pure QCD processes the contact interactions are a second important source of four–jet background events. All these background cross sections however are significantly smaller than the signal, as demonstrated in Fig. 5. This is also the case for the background from diagrams involving both QCD and contact interactions, with gluons in either the initial or the final state. The combinatorial background arising from the wrong three-jet combination in the jjj mass distribution is of the same order as the signal.

ℓ^* production. The possibility to create leptons copiously through contact interactions in pp collisions is one of the most exciting phenomena expected in composite models in which quarks and leptons have common constituents [5]. In this case also excited leptons could be produced in large numbers either singly via $q\bar{q} \to \ell\bar{\ell}^*$, $\ell^*\bar{\ell}$, or pairwise via $q\bar{q} \to \ell^*\bar{\ell}^*$ ($\ell = e,\ \nu$), Fig. 6. Background reactions to these channels are very rare in the Standard Model, and purely leptonic decays would provide very clear signatures for the experimental identification of excited electrons.

Summary. Excited quarks and leptons are produced with large cross sections in pp collisions once the threshold energy has been reached. This observation can be condensed in a few numbers by deriving the maximum excited quark and lepton masses accessible at the pp collider. As the discovery criterion we require that at least 100 signal events be observed within cuts. The discovery limits are summarized in the following table. For the LHC we considered two options: an integrated luminosity of 10^4 pb^{-1} and a "high luminosity" option with $4 \cdot 10^5$ pb^{-1}.

pp colliders turn out to be well suited for the search of excited quarks. Single q^* production is expected to be much larger than $q^*\bar{q}^*$ production. Clean and simple experimental signatures with small background are predicted for excited quarks which are produced via qg fusion and which decay via gauge interactions. Contact interactions may substantially enhance the q^* production cross section. This is reflected by the discovery limits for the LHC summarized in

Table 5

$\int \mathcal{L} dt$	LHC 10^4 pb^{-1}	LHC $4 \cdot 10^5$ pb^{-1}
q^* [G]	6.5 TeV	9.0 TeV
q^* [CT]	7.0 TeV	8.9 TeV
ℓ^* [CT]	4.0 TeV	5.6 TeV

the preceding table. If quarks and leptons share common subconstituents, even excited leptons could be produced copiously at this machine, producing spectacular lepton final states at very high rates.

Figure Captions

Fig. 1: Normalized χ-distributions for 2 jet cross sections at LHC (a) and SSC (b).

Fig. 2: Normalized χ-distributions for 3 jet cross sections at LHC (a) and SSC (b).

Fig. 3: Cross section for the production of excited quarks in quark-gluon fusion (solid line). The 2-jet QCD background is shown by the dashed line.

Fig. 4: Invariant mass distributions of excited quarks in the jj decay channel for various values of m* (dotted lines). The solid curve represents the QCD jj background.

Fig. 5: Cross section for the associated production of excited and ordinary quarks (solid line) with subsequent decay of the excited quark into three jets (contact interactions). The other curves show the four-jet background from QCD, contact interactions and diagrams involving both QCD and contact interactions.

Fig. 6: Cross sections for the associated production of ordinary and excited electrons (solid line) and e* pair production (dashed line).

References

[1] H. Harari, Proceedings of the 1984 Scottish Universities Summerschool, St. Andrews, Scotland.

[2] E. J. Eichten, K. D. Lane and M. I. Peskin, Phys. Rev. Lett. **50** (1983) 811.

[3] U. Baur, M. Spira and P. M. Zerwas, Phys. Rev. **D42** (1990) 815.

[4] P. Chiappetta and M. Perrottet, Preprint Marseille CPT-90/P.2440 (September 1990) to appear in Phys. Lett. B

[5] E. Eichten, I. Hinchliffe, K. Lane and C. Quigg, Rev. Mod. Phys. 56 (1984) 579.

[6] C. Bourrely, F.M. Renard, J. Soffer and P. Taxil, Phys. Rep. 177 (1989) 319.

[7] E.N. Argyres, C.G. Papadopoulos and S.D.P. Vlassopulos, Nucl. Phys. B324 (1989) 91.

[8] F. Aversa, P. Chiappetta, M. Greco and J.-Ph. Guillet, Phys. Rev. Lett. 65 (1990) 401; S.D. Ellis, Z. Kunszt and D.E. Soper, Phys. Rev. Lett. 64 (1990) 2121.

[9] M. Diemoz, F. Ferroni, E. Longo and G. Martinelli, Z. Phys. C39 (1988) 21.

[10] D.W. Duke and J.F. Owens, Phys. Rev. D30 (1984) 49.

[11] P. Méry, M. Perrottet and F.M. Renard, Z. Phys. C36 (1987) 249.

[12] P. Méry, S.E. Moubarik, M. Perrottet and F.M. Renard, Z. Phys. C46 (1990) 229.

[13] R. Rückl, in the Proceedings of the ECFA Workshop on LEP 200, CERN 87-08 (1987), Vol. II, p.453.

[14] P. Jenni, in the Proceedings of the ECFA Workshop on LEP 200, CERN 87-08 (1987), Vol. II, p.486.

[15] W.Buchmüller & D.Wyler, Nucl.Phys.**B268**(1986)621.

[16] E.N.Argyres & C.G.Papadopoulos: "Testing 3-boson couplings in the Standard Model via single W production at LEP", NCSR "Democritos" preprint, July 1990.

[17] R.Kleiss and W.J.Stirling, Nucl.Phys. **262**(1985)235.

[18] E.Eichten et *al.*, Rev.Mod.Phys.**56**(1984)579;**58**(1986)1065(E).

[19] E.N.Argyres, C.G.Papadopoulos & S.D.P. Vlassopulos, Nucl.Phys.**B324**(1989)91.

[20] U.Baur & E.W.N.Glover, Nucl. Phys. **B347**(1990) 12.

[21] R. Kleiss and P. Zerwas, Proceedings, Workshop *"Physics at Future Accelerators"*, La Thuile/CERN 1987.

[22] U. Baur, I. Hinchliffe and D. Zeppenfeld, Proceedings, Workshop *"From Colliders to Supercolliders"*, Madison (Wisconsin) 1987; Int. J. Mod. Phys. **A2** (1987) 1285.

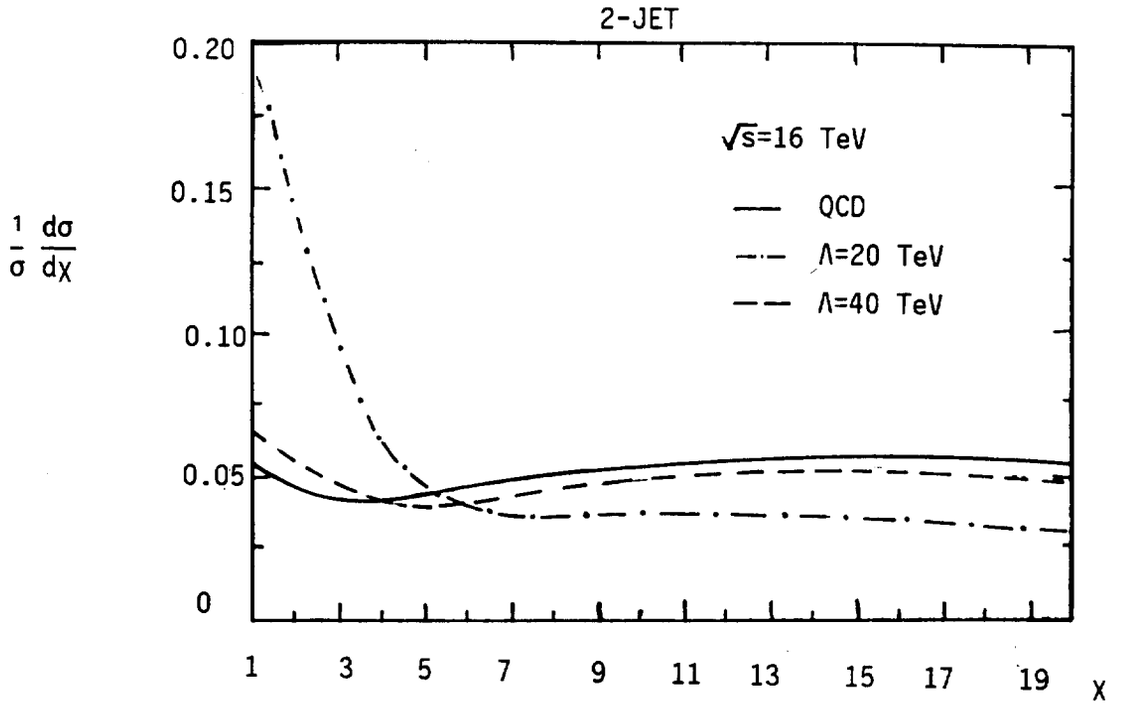
2-JET
0.20
0.15
0.10
0.05
0
√s=16 TeV
QCD
Λ=20 TeV
Λ=40 TeV
1
3
5
7
9
11
13
15
17
19
X
1/σ dσ/dχ

Fig.1a

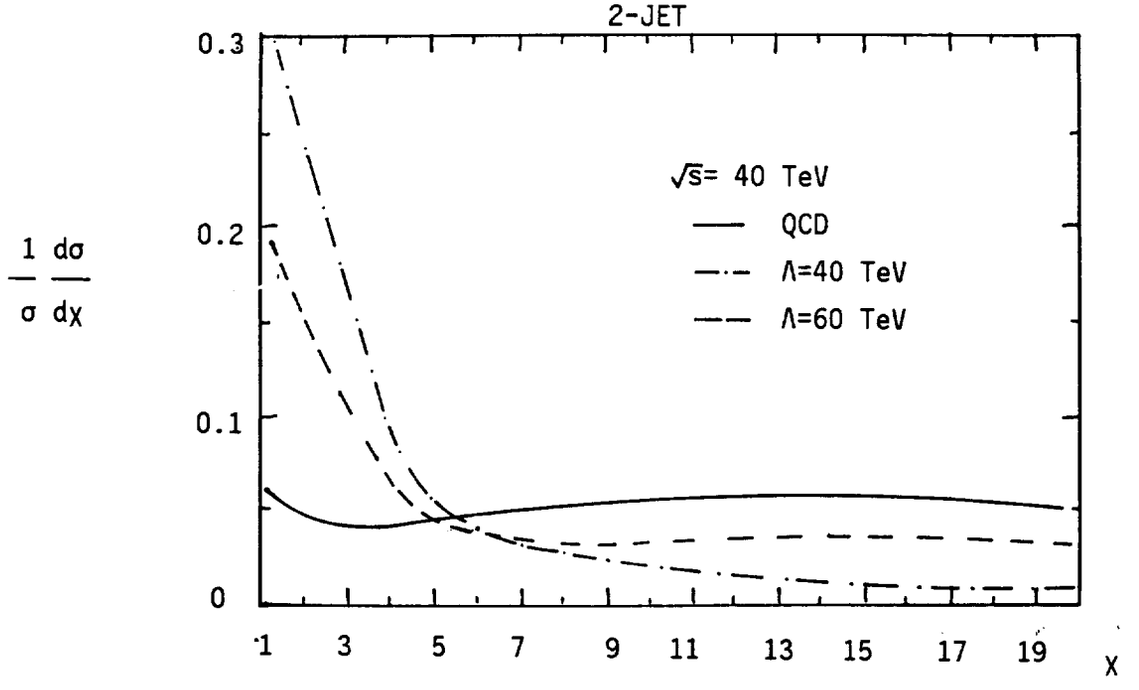
2-JET
0.3
0.2
0.1
0
√s= 40 TeV
QCD
Λ=40 TeV
Λ=60 TeV
1
3
5
7
9
11
13
15
17
19
X
1/σ dσ/dχ

Fig.1b

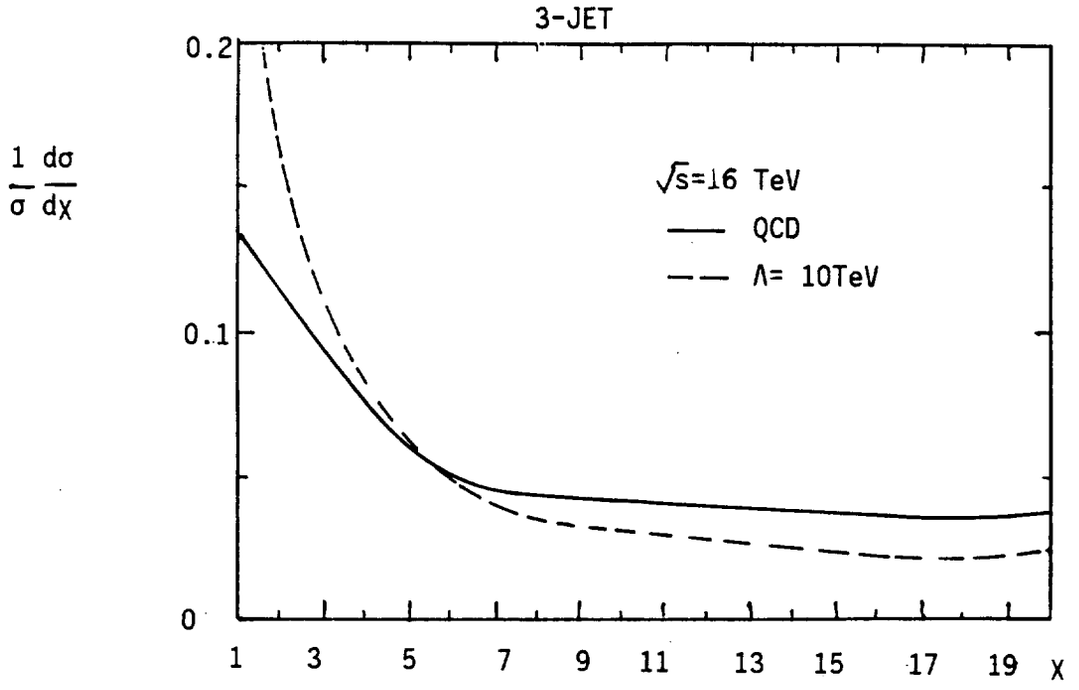
3-JET
$\frac{1}{\sigma}\frac{d\sigma}{dX}$
0.2
0.1
0
√s=16 TeV
QCD
Λ= 10TeV
1
3
5
7
9
11
13
15
17
19
X

Fig.2a

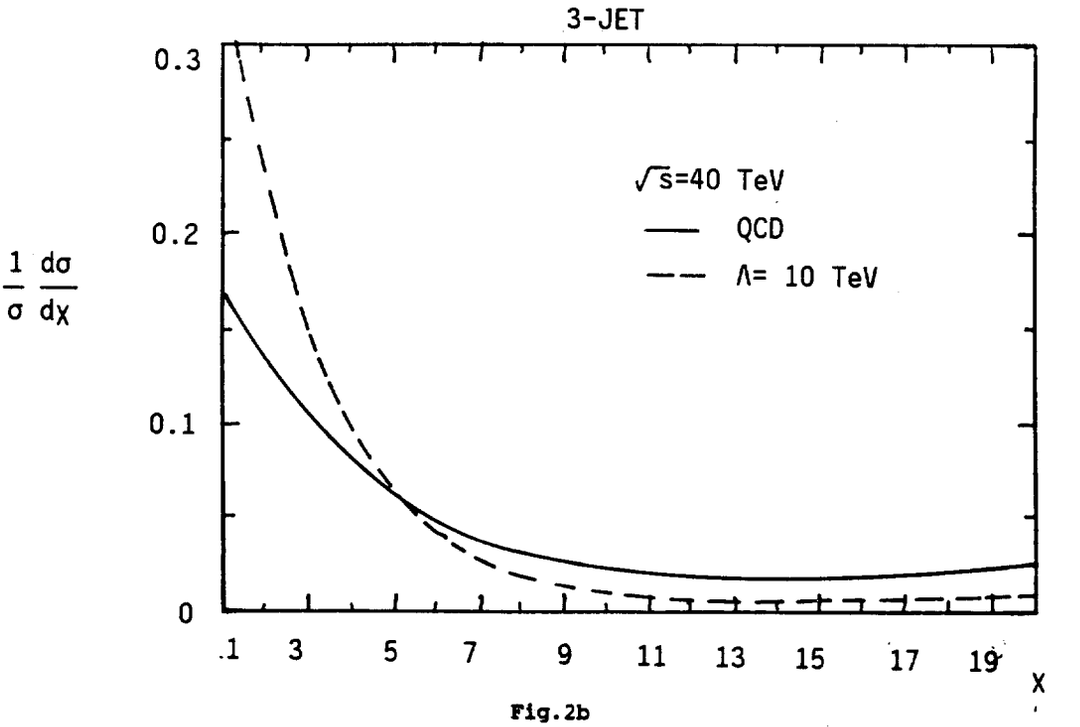
3-JET
$\frac{1}{\sigma}\frac{d\sigma}{dX}$
0.3
0.2
0.1
0
√s=40 TeV
QCD
Λ= 10 TeV
1
3
5
7
9
11
13
15
17
19
X

Fig.2b

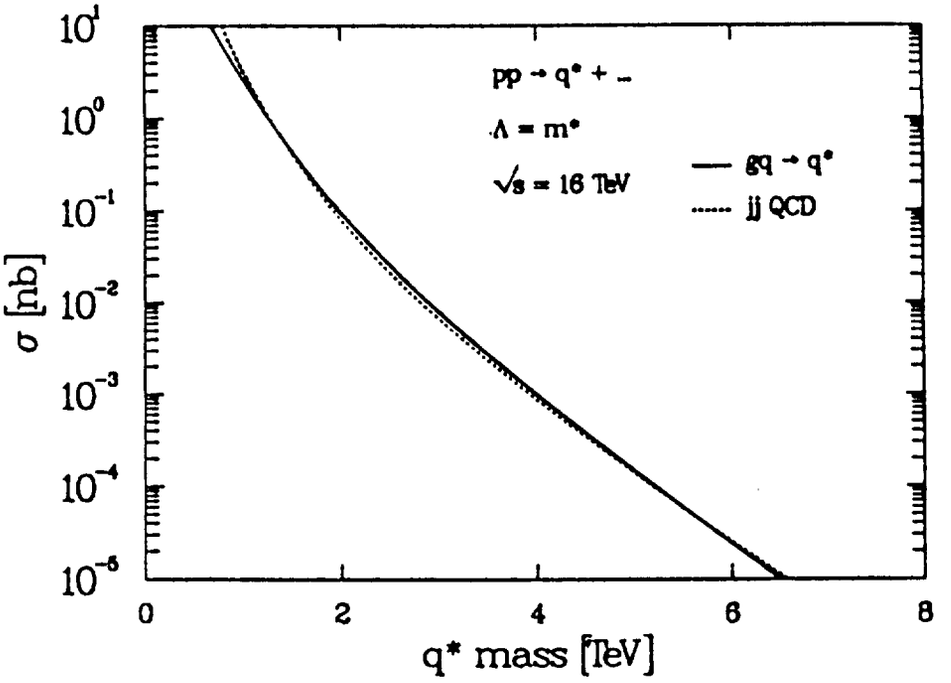
pp → q* + –
Λ = m*
√s = 16 TeV
gq → q*
jj QCD
σ [nb]
q* mass [TeV]

Fig. 3

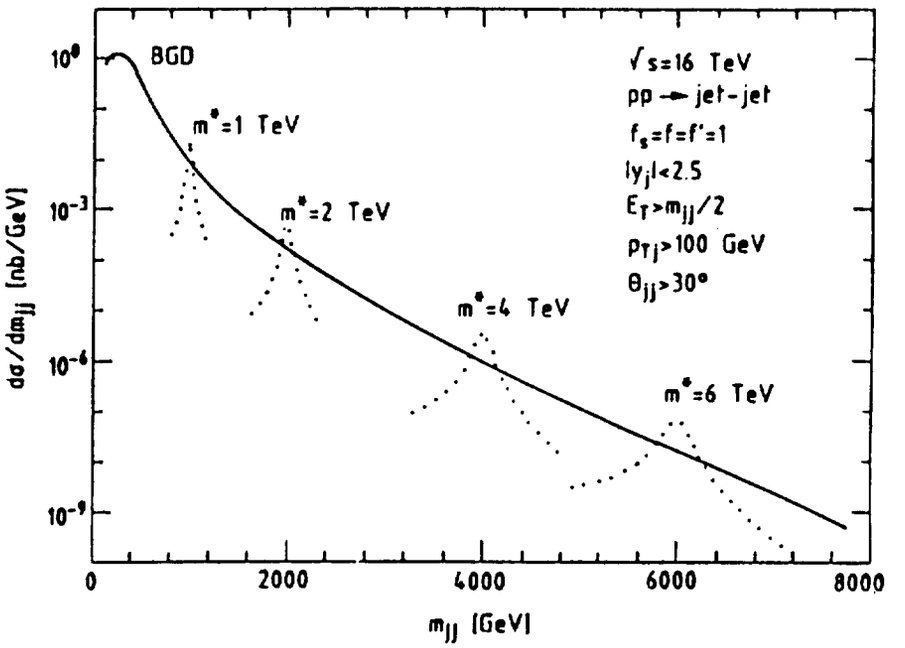
BGD
m*=1 TeV
m*=2 TeV
m*=4 TeV
m*=6 TeV
√s=16 TeV
pp → jet-jet
f_s=f=f'=1
|y_j|<2.5
E_T>m_jj/2
p_Tj>100 GeV
θ_jj>30°
dσ/dm_jj [nb/GeV]
m_jj [GeV]

Fig. 4

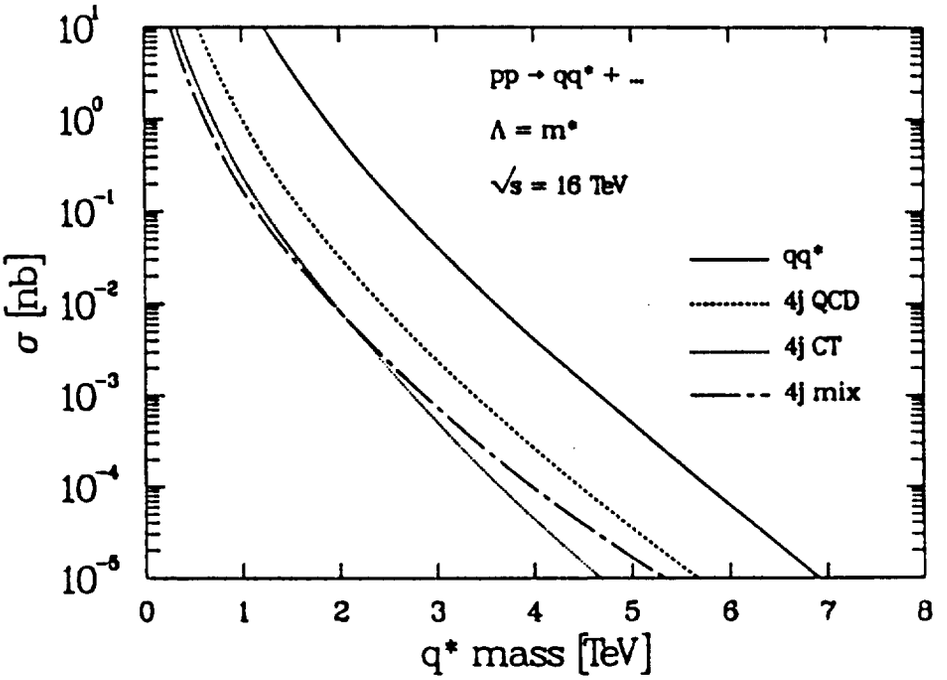
pp → qq* + ..
Λ = m*
√s = 16 TeV
qq*
4j QCD
4j CT
4j mix
σ [nb]
q* mass [TeV]

Fig. 5

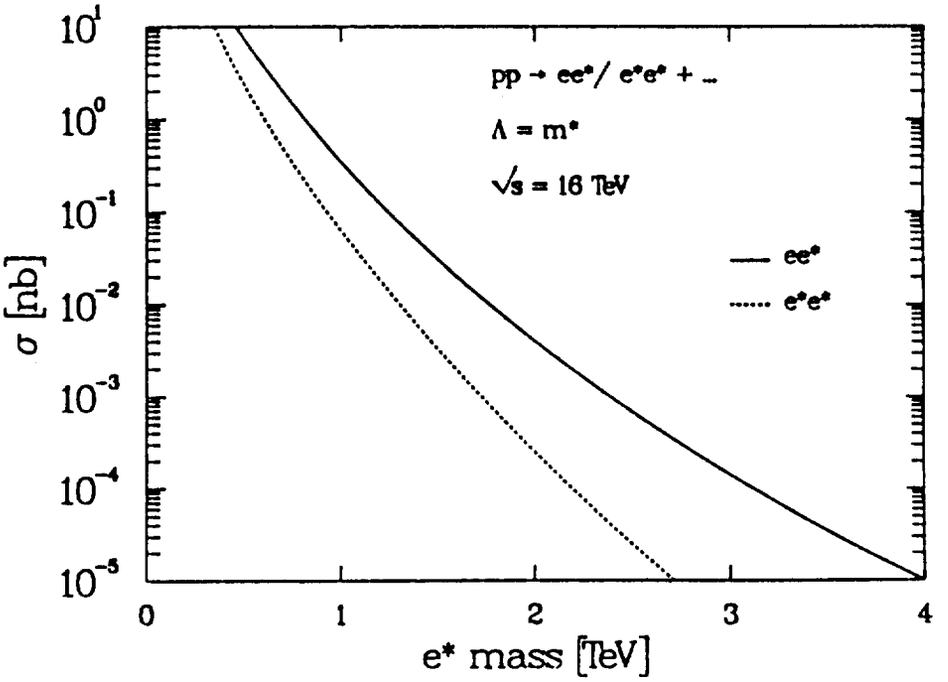
pp → ee*/ e*e* + ..
Λ = m*
√s = 16 TeV
ee*
e*e*
σ [nb]
e* mass [TeV]

Fig. 6